LINEAR SPACE-INVARIANT SYSTEM IDENTIFICATION AND MISMATCH BOUNDS FOR ESTIMATION OF DYNAMICAL IMAGES

Helmuth J. Naumer *Farzad Kamalabadi*

Department of Electrical and Computer Engineering and Coordinated Science Laboratory
University of Illinois at Urbana-Champaign

ABSTRACT

For linear space-invariant temporal systems, we provide a lower bound on the penalty incurred by approximating system dynamics in a Kalman filter by a random walk model, a common model when dynamics are unknown. We then present a computationally tractable algorithm for system identification of high-dimensional linear space-invariant dynamical systems, whereby the circulant structure of the state transition operator yields an estimate of the governing dynamics from a small number of temporal steps. By completing all operations in the frequency domain, we efficiently provide an estimate of the system dynamics and the state of the system. The estimation of system dynamics greatly improves the state estimation over the random walk model, suggesting classical estimators may remain applicable in modern imaging tasks.

Index Terms— Space-Invariant, Dynamical Systems, Model Mismatch, System Identification, Sequential Estimation

1. INTRODUCTION

In a wide range of image and video processing applications where frames are subject to temporal dynamics, recursive estimation has been used extensively with varying degrees of success [1, 2, 3]. Kalman filters have found particular success in the area of super-resolution (SR) video [4], due to the ease of explicitly modeling the downsampling process [5]. Additionally, Kalman filters have shown some success with estimating the optical flow used in other video processing algorithms [6, 7]. Recently, frequency domain calculations have shown success in deblurring due to the computational efficiency [8, 9]. As Kalman filters require a model of system dynamics, in video processing, a "random walk" system model is often used for state evolution when the true model is unknown [10, 11, 12], which would imply that every pixel follows on its own random walk, with no connection to its neighbors. Spatial information is typically incorporated separately [10, 13]. In such a model, each pixel changes without "consulting" its neighbors, then updates based on the neighbors within a single timestep; the model can be visualized as a 3D rectangular lattice. While such a model may preserve the relevant correlations, it is less physically motivated than the competing methods. In this paper, our spatiotemporal model has no direct connection within a given timestep, and any correlations come indirectly from other timesteps. In such a model, each adjacent pair of timesteps form a bipartite probabilistic graphical model, conducive to classic temporal methods.

As an example, in dynamic tomography, it has been shown that in some cases, approximating complicated dynamics by a random walk provides reasonable results, but there exists an unquantified gap in performance [12]. Due to the joint wide sense stationarity (WSS) of spatial random fields in tomography given a linear space invariant state transition operator, Kalman filter computations can be sped up dramatically to allow tractable estimation [14].

In this paper, we provide a lower bound on the performance gap between estimators using the correct linear system dynamics and the random walk approximation. Furthermore, we provide a computationally tractable joint estimator of system dynamics and image reconstruction. We show that by combining the frequency domain version of the Kalman filter [14], from here on referred to as the Kalman-Wiener Filter, with a new system identification method, we produce joint estimates of the system dynamics and associated minimum mean squared error (MMSE) estimates of the video.

The rest of the paper is organized as follows. Section 2 defines the signal model and section 3 provides an approximate lower bound on the mean squared error of a mismatched Kalman filter. Section 4 provides an estimator of space-invariant system dynamics using the observations directly. Section 5 provides numerical experiments of video de-noising and de-blurring of a small diffusion process. Concluding remarks are provided in section 6.

2. SIGNAL MODEL

The systems of interest in this work follow a standard linear state space model:

$$\mathbf{x}_{i+1} = \mathbf{F}_i \mathbf{x}_i + \mathbf{u}_i \tag{1}$$

$$\mathbf{y}_i = \mathbf{H}_i \mathbf{x}_i + \mathbf{v}_i \tag{2}$$

where $\mathbf{F}_i = \mathbf{F}$ is a constant linear state transition operator for all time indices i, resulting in time-invariant dynamics, and $\mathbf{H}_i$ is a linear measurement operator. $\mathbf{u}_i$ and $\mathbf{v}_i$ are sets of i.i.d centered Gaussian random vectors with covariance matrices $\mathbf{Q}$ and $\mathbf{R}$ respectively. Each vector in (1) and (2) are WSS spatial random fields as described in dynamic tomography [14]. The inner product on the associated Hilbert space is $\langle \mathbf{x}, \mathbf{y} \rangle = \mathbb{E}\left[\mathbf{x}^* \mathbf{y}\right]$, where $\mathbb{E}[X]$ denotes the expected value of X. The norm induced by the inner product is then $||\mathbf{x}|| = \sqrt{\mathbb{E}\left[|\mathbf{x}|^2\right]}$. Recall that the WSS constraint requires that for a given timestep, $\mathbb{E}[x_i(\mathbf{t})] = \mathbb{E}[x_i(\mathbf{s})]$ for all temporal indices i and spatial indices $\mathbf{s}, \mathbf{t}$. Finally, if we define the autocorrelation to be $R_{x_i,x_i}(\mathbf{s}, \mathbf{t}) = \langle x_i(\mathbf{s}), x_i(\mathbf{t}) \rangle$, the WSS constraint requires that $R_{x_i,x_i}(\mathbf{s}, \mathbf{t}) = R_{x_i,x_i}(\mathbf{s} - \mathbf{t}, \mathbf{0})$ for all temporal indices, i, and spatial indices, $\mathbf{s}$ and $\mathbf{t}$.

The Kalman filter is a classical method for providing estimates of the state of a linear dynamical system (LDS). It is formulated with two steps, a prediction step, and an update step, which take the forms

$$\hat{\mathbf{x}}_{i|i-1} = \mathbf{F}_i \hat{\mathbf{x}}_{i-1|i-1} \tag{3}$$

$$\hat{\mathbf{x}}_{i|i} = \hat{\mathbf{x}}_{i|i-1} + \mathbf{K}_i (\mathbf{y}_i - \mathbf{H}_i \mathbf{x}_{i|i-1}) \tag{4}$$

Authorized licensed use limited to: University of Illinois. Downloaded on June 21,2021 at 14:45:19 UTC from IEEE Xplore. Restrictions apply.

where $\hat{\mathbf{x}}_{i|j}$ is the MMSE estimate of $\mathbf{x}_i$ given $\{\mathbf{y}_i : 0 \leq i \leq j\}$, and $\mathbf{K}_i$ represents the model specific Kalman gain for timestep i.

3. MISMATCH IN SPACE-INVARIANT MODELS

In this section, we derive a lower bound on the performance discrepancy from model mismatch between the true system dynamics, and the random walk approximation. We construct the bound by showing that the error can be factored into a term identical to the ideal Kalman filter, but with the wrong gain, and an additional discrepancy term focused on the difference between the true state transition matrix and the identity matrix representing a random walk.

We begin our derivation by bounding the error of a single step of the mismatched Kalman filter. We then move to the steady state case.

Under the true signal model, the error from a single timestep given the previous state takes the form

$$\mathbf{e}_{\text{opt}} = \mathbf{K}(\mathbf{y}_{i+1} - \mathbf{H}_{i+1}\mathbf{F}\mathbf{x}_i) - \mathbf{u}_{i+1} \tag{5}$$
$$= \mathbf{K}(\mathbf{H}_{i+1}\mathbf{u}_{i+1} + \mathbf{v}_{i+1}) - \mathbf{u}_{i+1} \tag{6}$$

Under a mismatched state transition operator, $\mathbf{F}'$, the error becomes

$$\tilde{\mathbf{e}} = \mathbf{K}'_{i+1}(\mathbf{y}_{i+1} - \mathbf{H}_{i+1}\mathbf{F}'\mathbf{x}_i) - \mathbf{u}_{i+1} \tag{7}$$
$$= \left(\mathbf{K}'_{i+1}(\mathbf{H}_{i+1}\mathbf{u}_{i+1} + \mathbf{v}_{i+1}) - \mathbf{u}_{i+1}\right) + (\mathbf{I} - \mathbf{K}'_{i+1}\mathbf{H}_{i+1})\tilde{\mathbf{F}}\mathbf{x}_i \tag{8}$$

where $\tilde{\mathbf{F}} = \mathbf{F} - \mathbf{F}'$, $\mathbf{I}$ is the identity matrix, and $\mathbf{K}'_i$ is a perturbed version of the Kalman gain computed using the incorrect transition matrix. Because the first term is simply the error from the Kalman filter with a different gain term, we will give it a special notation

$$\tilde{\mathbf{e}}_{i,0} = \mathbf{K}'_{i+1}(\mathbf{H}_{i+1}\mathbf{u}_{i+1} + \mathbf{v}_{i+1}) - \mathbf{u}_{i+1} \tag{9}$$

As $\mathbf{x}_i$ is uncorrelated with future noise for all timesteps and the noise is assumed to be centered, the mean squared error reduces to

$$\text{mse} = ||\tilde{\mathbf{e}}_{i,0}||^2 + ||(\mathbf{I} - \mathbf{K}'_{i+1}\mathbf{H}_{i+1})\tilde{\mathbf{F}}\mathbf{x}_i||^2 \tag{10}$$
$$\geq \text{mse}_{\text{opt}} + ||(\mathbf{I} - \mathbf{K}'_{i+1}\mathbf{H}_{i+1})\tilde{\mathbf{F}}\mathbf{x}_i||^2 \tag{11}$$

where (11) comes from the fact that the Kalman filter and associated gain is optimal in the MSE sense, and thus, replacing $\mathbf{K}'$ with $\mathbf{K}$ reduces the norm. As a sanity check, it is easy to validate that if our observations are noiseless, we return to the MMSE of 0.

While the single step Kalman mismatch error is useful for understanding the source and form of the error, the ultimate quantity of interest is the steady state error. We anticipate some form of correlation decay, where we describe our finite time Kalman mismatch error as a transient error, and the asymptotic behavior to be steady state. To this effect, we denote the Kalman filter state estimate at time i using the incorrect gain $\mathbf{K}'$ to be $\hat{\mathbf{x}}'_{i|i}$ and the model mismatched state estimate to be $\tilde{\hat{\mathbf{x}}}_{i|i}$. Finally, we denote the discrepancy between the two estimates to be $\mathbf{d}_i = \hat{\mathbf{x}}'_{i|i} - \tilde{\hat{\mathbf{x}}}_{i|i}$.

Algebraically, it can be shown that, with $\mathbf{d}_0 = 0$,

$$\mathbf{d}_i = (\mathbf{I} - \mathbf{K}'_i\mathbf{H}_i)(\tilde{\mathbf{F}}\hat{\mathbf{x}}'_{i-1|i-1} + \mathbf{F}'\mathbf{d}_{i-1}) \tag{12}$$

By writing out the recursive relationship, we find that

$$\mathbf{d}_i = \sum_{j=0}^{i-1}\left(\prod_{k=i-1}^{j<i-1}(\mathbf{I} - \mathbf{K}'_i\mathbf{H}_i)\mathbf{F}'\right)(\mathbf{I} - \mathbf{K}'_j\mathbf{H}_j)\tilde{\mathbf{F}}\hat{\mathbf{x}}'_{j|j} \tag{13}$$

where the product term for $j = i - 1$ is equal to the identity and the indices of the product increase from right to left. Note that this discrepancy term takes the form that we expect, where the product forms the correlation decay (assuming a stable system), and we have the model mismatch from the single step version. Unfortunately, unlike the single step version, the discrepancy is no longer uncorrelated with the true Kalman error. Beginning with $\mathbf{e}_i = \mathbf{x}_i - \tilde{\hat{\mathbf{x}}}_{i|i} = \mathbf{e}_{i,0} + \mathbf{d}_i$, we proceed to look at the error:

$$||\mathbf{e}_i||^2 = ||\mathbf{e}_{i,0}||^2 + ||\mathbf{d}_i||^2 + 2\text{Re}\{\langle\mathbf{e}_{i,0}, \mathbf{d}_i\rangle\} \tag{14}$$
$$\geq \text{mse}_{\text{opt}} + ||\mathbf{d}_i||^2 + 2\text{Re}\{\langle\mathbf{e}_{i,0}, \mathbf{d}_i\rangle\} \tag{15}$$
$$e_{\text{gap}} \geq ||\mathbf{d}_i||^2 + 2\text{Re}\{\langle\mathbf{e}_{i,0}, \mathbf{d}_i\rangle\} \tag{16}$$

where $\mathbf{e}_{i,0}$ is the original form of the error from the Kalman filter, but with the suboptimal gain from the incorrect system model, and $e_{\text{gap}} = \|\mathbf{e}_i\|^2 - \text{mse}_{\text{opt}}$. Note that there exists a classical result for $||\mathbf{e}_{i,0}||^2$, despite our use of a potentially weak bound [15].

At this point, we start specializing this general form to the mismatch from the random walk model described in the introduction. We begin by looking at the error when $\mathbf{H}_i = \mathbf{H}$ and $\mathbf{F}' = \mathbf{I}$, which reduces the discrepancy term to

$$\mathbf{d}_i = \sum_{j=0}^{i-1}\left(\prod_{k=i-1}^{j<i-1}(\mathbf{I} - \mathbf{K}'_i\mathbf{H})\right)(\mathbf{I} - \mathbf{K}'_j\mathbf{H})\tilde{\mathbf{F}}\hat{\mathbf{x}}'_{j|j} \tag{17}$$

Combining the model with the definition in the Kalman filter,

$$\mathbf{K}'_i = \mathbf{P}_{i|i-1}\mathbf{H}^*(\mathbf{H}\mathbf{P}_{i|i-1}\mathbf{H}^* + \mathbf{R})^{-1} \tag{18}$$
$$\mathbf{P}_{i+1|i} = (\mathbf{I} - \mathbf{K}_i\mathbf{H})\mathbf{P}_{i|i-1} + \mathbf{Q} \tag{19}$$

Equations (18) and (19) fully define the evolution of the Kalman gain. $\mathbf{P}_{i|i-1}$ is the computed covariance matrix of the prediction error assuming the random walk model and given all $\mathbf{y}_j$ for $j \leq i-1$. Recalling our original model assumption that the noise is i.i.d. across time, every term in the equations can be computed element-wise in the frequency domain.

Using p^* and k^* to represent a fixed point of the scalar iteration for $\mathbf{P}$ and $\mathbf{K}$ respectively (representing a single frequency), r to be the scalar version of $\mathbf{R}$, q to be the scalar version of $\mathbf{Q}$, and h to be the scalar version of $\mathbf{H}$, we find the set of fixed points through solving the equation

$$\frac{p^{*2}|h|^2}{|h|^2p^* + r} = q \tag{20}$$

The solution of which implies fixed points at

$$p^* = \frac{q \pm \sqrt{q^2 + 4rq/|h|^2}}{2} \tag{21}$$

$$1 - k^*h = \frac{-1 + \sqrt{1 + \frac{4r}{|h|^2q}}}{1 + \sqrt{1 + \frac{4r}{|h|^2q}}} \tag{22}$$

where the positive p^* is chosen due to the PSD requirement on the matrix. By noting that $(1 - k^*h) \in [0, 1)$, we see that a summation of the power series of the term converges:

$$\sum_{i=0}^{\infty}(1 - k^*h)^i = \left(\frac{1 + \sqrt{1 + \frac{4r}{|h|^2q}}}{2}\right) \tag{23}$$

For convenience, we denote the linear operator representing the appropriate filtering applied by the result of the power series to be $\mathbf{D}$.

Authorized licensed use limited to: University of Illinois. Downloaded on June 21,2021 at 14:45:19 UTC from IEEE Xplore. Restrictions apply.

We are interested in the steady state error, and so we assume $k_i = k^*$ for the purpose of the bound. The discrepancy for large values of i becomes:

$$\mathbf{d}_i \approx \sum_{j=0}^{i-1} (\mathbf{I} - \mathbf{K}'\mathbf{H})^{i-j} \tilde{\mathbf{F}} \hat{\mathbf{x}}'_{j|j} \tag{24}$$

For sufficiently large i, such that the power summation for all separations of $\mathbf{x}'_{i|i}$ are either sufficiently uncorrelated, or the summation can be approximated by our filter $\mathbf{D}$:

$$||\mathbf{d}_i||^2 \approx \sum_{j=0}^{i-1} \langle \mathbf{D}\tilde{\mathbf{F}}\hat{\mathbf{x}}'_{i|i}, \mathbf{D}\tilde{\mathbf{F}}\hat{\mathbf{x}}'_{i-j|i-j} \rangle \tag{25}$$

By using the transformation between estimate timesteps and removing orthogonal terms, we can write:

$$\begin{aligned} \langle \hat{\mathbf{x}}'_{i-j|i-j}, \hat{\mathbf{x}}'_{i|i} \rangle = \; & \langle \hat{\mathbf{x}}'_{i-j|i-j}, (\mathbf{I} - \mathbf{K}'\mathbf{H})^j \hat{\mathbf{x}}'_{i-j|i-j} \rangle \\ & + \langle \hat{\mathbf{x}}'_{i-j|i-j}, \mathbf{K}\mathbf{H}\mathbf{F}^j \mathbf{x}_{i-j} \rangle \end{aligned} \tag{26}$$

$$||\mathbf{d}_i||^2 \approx \sum_{j=0}^{i-1} ||\mathbf{D}\tilde{\mathbf{F}}(\mathbf{I} - \mathbf{K}'\mathbf{H})^j \hat{\mathbf{x}}'_{i|i}||^2 + \langle \mathbf{D}\tilde{\mathbf{F}}\hat{\mathbf{x}}'_{i|i}, \mathbf{D}\tilde{\mathbf{F}}\mathbf{K}'\mathbf{H}\mathbf{F}^j \mathbf{x}_i \rangle \tag{27}$$

We now set up an iteration for the cross terms between our gain-perturbed estimate and the true state. If we define $\mathbf{P}_{i,c} = \mathbb{E}[\hat{\mathbf{x}}'_{i|i}\mathbf{x}_i^\top]$, and $\mathbf{P}_i = \mathbb{E}[\mathbf{x}_i\mathbf{x}_i^\top]$

$$\begin{aligned} \mathbf{P}_{i,c} &= \mathbb{E}[(\mathbf{I} - \mathbf{K}'\mathbf{H})\mathbf{F}\hat{\mathbf{x}}_{i-1|i-1}(\mathbf{F}\mathbf{x}_{i-1})^\top] && (28) \\ &\quad + \mathbf{K}'\mathbf{H}\mathbb{E}[\mathbf{x}_i\mathbf{x}_i^\top] && (29) \\ &= (\mathbf{I} - \mathbf{K}'\mathbf{H})\mathbf{F}\mathbf{P}_{i-1,c}\mathbf{F}^\top + \mathbf{K}'\mathbf{H}\mathbf{P}_i && (30) \end{aligned}$$

Continuing the steady state approximation, $\mathbf{P}_i$ can be treated as a constant input computed separately from the true system dynamics. Continuing our theme of linear space invariance enabling a scalar iteration in the frequency domain, noting that $\mathbf{x}_i = \sum_{j=0}^{i} \mathbf{F}^{i-j}\mathbf{u}_j$, and that each $\mathbf{u}_j$ is orthogonal to each other, each point in the frequency domain can be computed as

$$\begin{aligned} p_i &= p_u \sum_{j=0}^{i} |f|^{2j} && (31) \\ &\approx \frac{p_u}{1 - |f|^2} && (32) \end{aligned}$$

Substituting in (32), our cross term iteration in the frequency domain then becomes

$$\begin{aligned} p_{i,c} &= (1 - k'h)|f|^2 p_{i-1,c} + \frac{k'hp_u}{1 - |f|^2} && (33) \\ &\approx \frac{k'hp_u}{(1 - (1 - k'h)|f|^2))(1 - |f|^2)} && (34) \end{aligned}$$

where equations (32) and (34) come from approximating the finite sum as infinite to model steady state behavior.

Finally, we set up the iteration of the power spectral density of the estimate itself, where $\hat{\mathbf{P}}_i = \mathbb{E}[\hat{\mathbf{x}}'_{i|i}\hat{\mathbf{x}}'^\top_{i|i}]$. First note the recursive formula for the estimate:

$$\hat{\mathbf{x}}'_{i|i} = (\mathbf{I} - \mathbf{K}'\mathbf{H})\mathbf{F}\hat{\mathbf{x}}_{i-1|i-1} + \mathbf{K}'\mathbf{H}\mathbf{x}_i + \mathbf{K}'\mathbf{v}_i \tag{35}$$

From here we find a recursion for the covariance matrix. By removing orthogonal terms, we set up the iteration:

$$\begin{aligned} \hat{\mathbf{P}}_i = & (\mathbf{I} - \mathbf{K}'\mathbf{H})\mathbf{F}\hat{\mathbf{P}}_{i-1}\mathbf{F}^\top(\mathbf{I} - \mathbf{K}'\mathbf{H})^\top \\ & + \mathbf{K}'\mathbf{P}_v\mathbf{K}'^\top \\ & + \mathbf{K}'\mathbf{H}\mathbf{P}_i\mathbf{H}^\top\mathbf{K}'^\top \\ & + 2(\mathbf{I} - \mathbf{K}'\mathbf{H})\mathbf{F}\mathbf{P}_{i,c}\mathbf{F}' \end{aligned} \tag{36}$$

Converting to a scalar iteration as before

$$\begin{aligned} \hat{p}_i = \; & |(1 - k'h)f|^2 \hat{p}_{i-1} \\ & + |k'|^2(p_v + |h|^2 p_i) \\ & + 2(1 - k'h)|f|^2 p_{i,c} \end{aligned} \tag{37}$$

and doing one final steady state approximation, we find

$$\hat{p}_i \approx \frac{|k'|^2(p_v + |h|^2 p_i) + 2(1 - k'h)|f|^2 p_{i,c}}{1 - |(1 - k'h)f|^2} \tag{38}$$

Now, plugging all of our intermediate results into (27):

$$\begin{aligned} ||\mathbf{d}_i||^2 \approx \sum_{j=0}^{i-1} \mathrm{Tr}(& (\mathbf{I} - \mathbf{K}'\mathbf{H})^{j\top} \tilde{\mathbf{F}}^\top \mathbf{D}^\top \mathbf{D}\tilde{\mathbf{F}}(\mathbf{I} - \mathbf{K}'\mathbf{H})^j \hat{\mathbf{P}}_i \\ & + \tilde{\mathbf{F}}^\top \mathbf{D}^\top \mathbf{D}\tilde{\mathbf{F}}\mathbf{K}'\mathbf{H}\mathbf{F}^j \mathbf{P}_{i,c}) \end{aligned} \tag{39}$$

This term is the sum over all of the frequency components, and the representation of a single element is:

$$d_e \approx |d|^2 |\tilde{f}|^2 \sum_{j=0}^{i-1} |(1 - k'h)|^{2j} \hat{p}_i + k'hf^j p_{i,c} \tag{40}$$

$$d_e \approx |d|^2 |\tilde{f}|^2 \left(\frac{\hat{p}_i}{1 - |(1 - k'h)|^2} + \frac{k'hp_{i,c}}{1 - f} \right) \tag{41}$$

Now that we have all of the intermediate results, the original cross term is easier to derive.

$$\begin{aligned} \langle \mathbf{e}_{i,0}, \mathbf{d}_i \rangle &= \langle \hat{\mathbf{x}}'_{i|i} - \mathbf{x}_i, \mathbf{d}_i \rangle && (42) \\ &\approx \sum_{j=0}^{i-1} \langle \hat{\mathbf{x}}'_{i|i} - \mathbf{x}_i, (\mathbf{I} - \mathbf{K}'\mathbf{H})^{i-j} \tilde{\mathbf{F}} \hat{\mathbf{x}}'_{j|j} \rangle && (43) \\ &= \sum_{j=0}^{i-1} \langle -\mathbf{F}^{i-j}\mathbf{x}_j, (\mathbf{I} - \mathbf{K}'\mathbf{H})^{i-j} \tilde{\mathbf{F}} \hat{\mathbf{x}}'_{j|j} \rangle \\ &\quad + \langle \mathbf{K}\mathbf{H}\mathbf{F}^{i-j}\mathbf{x}_j, (\mathbf{I} - \mathbf{K}'\mathbf{H})^{i-j} \tilde{\mathbf{F}} \hat{\mathbf{x}}'_{j|j} \rangle \\ &\quad + \langle (\mathbf{I} - \mathbf{K}'\mathbf{H})^{i-j} \hat{\mathbf{x}}'_{j|j}, (\mathbf{I} - \mathbf{K}'\mathbf{H})^{i-j} \tilde{\mathbf{F}} \hat{\mathbf{x}}'_{j|j} \rangle && (44) \end{aligned}$$

Each element in the frequency domain takes the form

$$2 \left(\frac{\tilde{f}\hat{p}_i}{1 - |1 - k'h|^2} - \frac{(1 - k'h)\tilde{f}p_{i,c}}{1 - (1 - k'f)f^*} \right) \tag{45}$$

None of the operations break the conjugate symmetry, so (45) doesn't require any modification to take the real part in the spatial domain. Thus, the performance gap is simply the sum of (45) and (41) for each element in the frequency domain, and then summed over the entire frequency domain.

Authorized licensed use limited to: University of Illinois. Downloaded on June 21,2021 at 14:45:19 UTC from IEEE Xplore. Restrictions apply.

The bound can provide most insight by observing relative contributions of terms. As an example, consider all $(1 - k'h)$ under large measurement noise to be approximately 1. For this reason, we may want to consider the terms with a denominator of the form $1 - |1 - k'h|^2$ to be more dominant in general. Such an approximation would produce an error at each frequency

$$e_{\text{gap}} \approx \left(\frac{|d|^2 |\tilde{f}|^2 + 2\tilde{f}}{1 - |1 - k'h|^2} \right) \hat{p}_i \tag{46}$$

where

$$\hat{p}_i \approx \left(\frac{|k'|^2}{1 - |f|^2} \right) p_v + \left(\frac{2|f|^2 k'h + |k'h|^2}{(1 - |f|^2)^3} \right) p_u \tag{47}$$

From this approximation, it can be seen that model mismatch can produce a significant penalty at every frequency as a quadratic function of the model discrepancy. In the next section, we provide a method to reduce this gap directly from the measurements.

4. SYSTEM IDENTIFICATION

In this section, we derive an estimator for the system dynamics directly from the measurements for a linear space-invariant system. We do this by defining the iteration to step from one measurement to the next, then solving for the transition operator as a function of the power spectral densities and cross spectral densities. We denote the power spectral density of a WSS random field $\mathbf{W}$ as $S_{W,W}$.

By noting that our measurement and state transition operators commute, an inexpensive estimate of the system dynamics can be found directly from the observations. By stepping through a single timestep from $\mathbf{y}_i$ to $\mathbf{y}_{i+1}$, we find the transition can be represented directly as

$$\mathbf{y}_{i+1} = \mathbf{H}(\mathbf{F}\mathbf{H}^{-1}(\mathbf{y}_i - \mathbf{v}_i) + \mathbf{u}_i) + \mathbf{v}_{i+1} \tag{48}$$

$$= \mathbf{F}\mathbf{y}_i - \mathbf{F}\mathbf{v}_i + \mathbf{v}_{i+1} + \mathbf{H}\mathbf{u}_i \tag{49}$$

If we assume some initial $\mathbf{y}_0 = \mathbf{H}\mathbf{u}_0 + \mathbf{v}_0$, then

$$\mathbf{y}_i = \mathbf{v}_i + \sum_{i=0}^{n} \mathbf{F}^{n-i} \mathbf{H} \mathbf{u}_i \tag{50}$$

Assuming WSS, the power spectral density of $\mathbf{y}_i$ is then

$$S_{Y_i,Y_i} = S_{V,V} + \sum_{j=0}^{i} \mathbf{F}^{*i-j} \mathbf{F}^{i-j} \mathbf{H}^* \mathbf{H} S_{U,U} \tag{51}$$

and the cross spectral density between $\mathbf{y}_i, \mathbf{y}_{i+1}$ is

$$S_{Y_i,Y_{i+1}} = \sum_{j=0}^{i} \mathbf{F}^{*i-j} \mathbf{F}^{i+1-j} \mathbf{H}^* \mathbf{H} S_{U,U} \tag{52}$$

$$= \mathbf{F}(S_{Y_i,Y_i} - S_{V,V}) \tag{53}$$

Thus we propose an estimator of the form:

$$\hat{F}(\mathbf{f}) = \frac{\sum_i \hat{S}_{Y_i,Y_{i+1}}(\mathbf{f})}{\sum_i (\hat{S}_{Y_i,Y_i}(\mathbf{f}) - S_{V,V}(\mathbf{f}))} \tag{54}$$

where $\hat{S}_{Y_i,Y_{i+1}}$ and $\hat{S}_{Y_i,Y_i}$ are the empirical spectral densities. A detailed analysis of the estimator is beyond the scope of this paper, and is left to future work. It can be shown that the estimator has relationships with Linear Inverse Modeling [16, 17, 18] and thus Dynamic Mode Decomposition [19, 20].

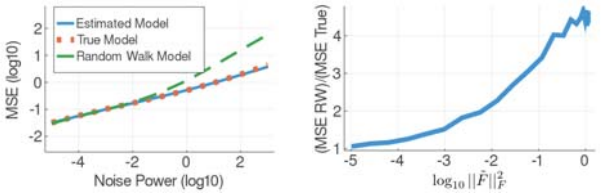

Fig. 1. Left: Mean Squared Error as a function of measurement noise, ratio equal for ease of viewing slopes; Right: Ratio of error with random walk model and true model varying diffusion rate.

5. NUMERICAL EXPERIMENTS

In this section, we describe results of numerical experiments. We simulated diffusion with various noise powers and diffusion rates.

The Kalman-Wiener filter and our system identification algorithm were both implemented in Julia 1.2.0. The Kalman-Wiener filter was simulated with the correct model, an independent random walk model of the system, and the estimated system model. The true state transition operator was a diffusion operation with a small amount of drift. The convolutional kernel was

$$\text{kernel} \propto \begin{bmatrix} 0.25 & 0.5 & 0.25 \\ 0.5 & a & 0.5 \\ 0.25 & 0.5 & 0.25 \end{bmatrix} \tag{55}$$

shifted to the right by one sample and normalized such that a conservation of mass principle is followed. That is to say, the sum of the terms is equal to 1. 20 timesteps were simulated, with iid gaussian noise of power 1 added to the state at each timestep. The image was initialized at 0 then simulated until clusters formed. Additionally, the measurement operator was a 5×5 centered square convolution kernel blurring the image. Mean squared error was evaluated on the final timestep.

In one experiment, $a = 1$ was fixed and the measurement noise power was sweeped. The mean squared error results of the simulations are available in the left panel of figure 1. We see that, as expected, for small amounts of noise, there is no benefit to having a good model, as the Kalman filter directly incorporates the measurement and ignores the transitions. For moderate amounts of noise, the joint estimation technique outperforms the random walk model, providing almost equivalent performance to the true model.

Additionally, a set of simulations were done maintaining a fixed level of measurement noise power of 1 with no drift while varying the rate of diffusion, and thus the distance from a random walk model. In the right panel of figure 1, we show the ratio of mean squared error between random walk model estimation and the true model estimation as a function of the Frobenius norm of the difference between the true model and the random walk model.

We additionally simulated other blurring measurement operators and found similar results, though they are not included in this paper due to space constraints.

6. CONCLUSION

This work suggests that classically optimal estimators may still be useful for some imaging tasks when combined with simple system identification methods, despite the comparatively poor performance caused by model mismatch. The model estimate greatly improves the state estimation over the random walk model, helping to close the derived performance gap induced by model mismatch.

Authorized licensed use limited to: University of Illinois. Downloaded on June 21,2021 at 14:45:19 UTC from IEEE Xplore. Restrictions apply.

7. REFERENCES

[1] Georgios Stamou, Michail Krinidis, Evangelos Loutas, Nikos Nikolaidis, and Ioannis Pitas, "4.11 - 2D and 3D Motion Tracking in Digital Video," in *Handbook of Image and Video Processing (Second Edition)*, AL BOVIK, Ed., Communications, Networking and Multimedia, pp. 491 – XVIII. Academic Press, Burlington, second edition edition, 2005.

[2] J. Scott, M. A. Pusateri, and D. Cornish, "Kalman filter based video background estimation," in *2009 IEEE Applied Imagery Pattern Recognition Workshop (AIPR 2009)*, Oct 2009, pp. 1–7.

[3] Ohyun Kwon, Jeongho Shin, and Joonki Paik, "Video Stabilization Using Kalman Filter and Phase Correlation Matching," in *Image Analysis and Recognition*, Mohamed Kamel and Aurélio Campilho, Eds., Berlin, Heidelberg, 2005, pp. 141–148, Springer Berlin Heidelberg.

[4] S. Farsiu, M.D. Robinson, M. Elad, and P. Milanfar, "Fast and robust multiframe super resolution," *IEEE Transactions on Image Processing*, vol. 13, no. 10, pp. 1327–1344, Oct. 2004.

[5] Sina Farsiu, Dirk M. Robinson, Michael Elad, and Peyman Milanfar, "Dynamic demosaicing and color superresolution of video sequences," in *Image Reconstruction from Incomplete Data III*. Oct. 2004, vol. 5562, pp. 169–178, International Society for Optics and Photonics.

[6] Wenbo Bao, Xiaoyun Zhang, Li Chen, and Zhiyong Gao, "KalmanFlow: Efficient Kalman Filtering for Video Optical Flow," in *2018 25th IEEE International Conference on Image Processing (ICIP)*, Oct. 2018, pp. 3343–3347, ISSN: 2381-8549.

[7] Wenbo Bao, Xiaoyun Zhang, Li Chen, and Zhiyong Gao, "KalmanFlow 2.0: Efficient Video Optical Flow Estimation via Context-Aware Kalman Filtering," *IEEE Transactions on Image Processing*, vol. 28, no. 9, pp. 4233–4246, Sept. 2019.

[8] Mauricio Delbracio and Guillermo Sapiro, "Hand-Held Video Deblurring Via Efficient Fourier Aggregation," *IEEE Transactions on Computational Imaging*, vol. 1, no. 4, pp. 270–283, Dec. 2015.

[9] Mauricio Delbracio and Guilermo Sapiro, "Burst deblurring: Removing camera shake through fourier burst accumulation," in *2015 IEEE Conference on Computer Vision and Pattern Recognition (CVPR)*, June 2015, pp. 2385–2393, ISSN: 1063-6919.

[10] R. Dugad and N. Ahuja, "Video denoising by combining kalman and wiener estimates," in *Proceedings 1999 International Conference on Image Processing (Cat. 99CH36348)*, Oct 1999, vol. 4, pp. 152–156 vol.4.

[11] Thibaud Ehret, Jean-Michel Morel, and Pablo Arias, "Non-Local Kalman: A Recursive Video Denoising Algorithm," in *2018 25th IEEE International Conference on Image Processing (ICIP)*, Oct. 2018, pp. 3204–3208, ISSN: 2381-8549.

[12] Mark D. Butala, Richard A. Frazin, Yuguo Chen, and Farzad Kamalabadi, "Tomographic Imaging of Dynamic Objects With the Ensemble Kalman Filter," *IEEE Transactions on Image Processing*, vol. 18, no. 7, pp. 1573–1587, July 2009.

[13] Pablo Arias and Jean-Michel Morel, "Kalman filtering of patches for frame-recursive video denoising," in *The IEEE Conference on Computer Vision and Pattern Recognition (CVPR) Workshops*, June 2019.

[14] Mark D. Butala and Farzad Kamalabadi, "Optimal dynamic tomography for wide-sense stationary spatial random fields," in *2009 16th IEEE International Conference on Image Processing (ICIP)*, Nov. 2009, pp. 593–596, ISSN: 2381-8549.

[15] H. Heffes, "The effect of erroneous models on the Kalman filter response," *IEEE Transactions on Automatic Control*, vol. 11, no. 3, pp. 541–543, July 1966.

[16] Cecile Penland, "Random Forcing and Forecasting Using Principal Oscillation Pattern Analysis," *Mon. Wea. Rev.*, vol. 117, no. 10, pp. 2165–2185, Oct. 1989.

[17] Cécile Penland and Theresa Magorian, "Prediction of Niño 3 Sea Surface Temperatures Using Linear Inverse Modeling," *J. Climate*, vol. 6, no. 6, pp. 1067–1076, June 1993.

[18] Cécile Penland and Prashant D. Sardeshmukh, "The Optimal Growth of Tropical Sea Surface Temperature Anomalies," *J. Climate*, vol. 8, no. 8, pp. 1999–2024, Aug. 1995.

[19] P.J. Schmid, "Dynamic mode decomposition of numerical and experimental data," *Journal of Fluid Mechanics*, vol. 656, pp. 5–28, 2010, 5.

[20] Jonathan H. Tu, Clarence W. Rowley, Dirk M. Luchtenburg, Steven L. Brunton, and J. Nathan Kutz, "On dynamic mode decomposition: Theory and applications," *Journal of Computational Dynamics*, vol. 1, no. 2, pp. 391, 2014.

Authorized licensed use limited to: University of Illinois. Downloaded on June 21,2021 at 14:45:19 UTC from IEEE Xplore. Restrictions apply.